

Microfluidic Devices as Gas – Ionic Liquid Membrane Contactors for CO₂ Removal from Anaesthesia Gases

M. Malankowska^{a,b,c}, C.F. Martins^b, H.S. Rho^c, L.A. Neves^b, R.M. Tiggelaar^c, J.G. Crespo^b, M.P. Pina^{a,d*}, R. Mallada^{a,d}, H. Gardeniers^c, I.M. Coelho^{b*}

^aInstitute of Nanoscience of Aragon, Department of Chemical & Environmental Engineering, University of Zaragoza, Edif. I+D+i, Campus Rio Ebro, C/Mariano Esquillor, 50018 Zaragoza, Spain.

^bLAQV/REQUIMTE, Departamento de Química, Faculdade de Ciências e Tecnologia, Universidade NOVA de Lisboa, 2829-516 Caparica, Portugal

^cMesoscale Chemical Systems, MESA+ Institute for Nanotechnology, University of Twente, P.O. Box 217, 7500 AE Enschede. The Netherlands.

^dNetworking Research Centre on Bioengineering, Biomaterials and Nanomedicine, CIBER-BBN, 28029 Madrid, Spain.

*corresponding authors: mapina@unizar.es; imrc@fct.unl.pt

Abstract

This work proposes a microfluidic gas – ionic liquid contactor for CO₂ removal from anaesthesia gas, containing Xe. The working principle involves the transport of CO₂ through a polymer flat membrane followed by its capture and enzymatic bioconversion in the ionic liquid solvent. Microfluidic devices enable a rapid and inexpensive screening of potential CO₂ absorbers. The alveolar – type design of the ionic liquid chamber was adopted to reduce mass transfer limitations of CO₂ through the liquid phase. Polydimethylsiloxane (PDMS) was the chosen polymer for dense membrane, as well as for the microfluidic device fabrication, mainly due to the high permeability of gases, O₂ and CO₂, and low cost. The selected ionic liquid was cholinium propionate (CP) with a water activity of 0.753, due to its high affinity towards CO₂ and biocompatibility with the enzyme used for CO₂ conversion to bicarbonate, carbonic anhydrase (CA).

The CO₂ and Xe permeability and CO₂/Xe selectivity were determined in the microfluidic devices developed and compared to those exhibited by free standing PDMS membranes mounted on a standard permeation cell. The performance of the microfluidic devices as gas – ionic liquid contactors was evaluated for a given solvent flow rate with pure gas streams of CO₂ and Xe. The obtained results show that cholinium propionate with or without the enzyme has no effect on the Xe transport, but remarkably enhances the affinity

towards carbon dioxide leading to enhancement factor up to 1.9 in the presence of 0.1 mg CA/gIL.

Keywords: Carbon dioxide removal, Anaesthesia gas recovery, Microfluidic membrane contactor, Cholinium-based ionic liquids, Carbonic anhydrase enzyme.

1. Introduction

The most commonly used anaesthetic gas for surgical operations is nitrous oxide (N_2O). The mixture of nitrous oxide and volatile anaesthetic compounds, mainly isoflurane, desflurane and sevoflurane, is introduced to the closed breathing system [1]. The main problem with such mixture is the risk of hypoxia. Hypoxia caused by the excessive amount of N_2O , also called a ‘third gas effect’, influences the partial pressure of O_2 within the alveolar channels. When high quantity of nitrous oxide is present in the alveoli, O_2 and CO_2 are diluted by this gas which leads to the decrease of their respective partial pressures resulting in insufficient blood oxygenation [2].

An alternative approach in order to replace nitrous oxide is to use Xe as an anaesthetic gas. The anaesthetic properties of Xe were discovered, analysed and described in the early 1950s [3]. Xe possesses a number of characteristics that make it a perfect anaesthetic compound. It is hemodynamically stable, which results in lack of cardiac depression, it produces high regional blood flow and it possesses low solubility in liquids, greatly reducing the risk of hypoxia [2, 4]. Xe is particularly attractive for the neonates as it attenuates isoflurane neurotoxicity [5]. Moreover, Xe is non – flammable, non – toxic, and does not contribute to the depletion of the ozone layer [2, 6] compared to N_2O ; however, it is far more expensive (1 litre of produced liquid Xe consumes 792 kJ which costs approximately 1000 \$, that is 100 times more than the price of N_2O) [4, 6]. Hence, recycling of Xe from the anaesthesia exhaled gas rather than wasting it to the atmosphere is the only way to ensure economic and efficient Xe use.

The gas mixture exhaled from the patient during the surgical operation, where Xe is used as an anaesthetic gas, consists mainly of Xe ($\approx 65\%$), O_2 ($\approx 27\%$), N_2 ($\approx 3.3\%$) and CO_2 (5%) [1]. The conventional method of removing CO_2 from the exhaled gas mixture in a closed – circuit technology relies on the use of soda lime that is composed of: calcium hydroxide, water, sodium hydroxide and potassium hydroxide. In this system the removal of CO_2 is limited by the size of the CO_2 absorber canister [5]. Apart from this, the process is relatively efficient and commonly used, but it suffers from a number of problems. The soda lime, if allowed to dry up, can produce hydrogen and heat resulting in an explosion hazard; or can

react with volatile anaesthetic compounds producing toxic side products (e.g. fluoromethyl-1-2,2-difluoro-a-(trifluoromethyl) vinyl ether [7] or carbon monoxide [1]) in the gas circuit. Therefore, several attempts, with alternative methods, are being investigated for the on – line removal of CO₂ from anaesthetic closed circuits down to 0.5%. Mendes *et al* proposed the use of a membrane contactor technology with commercial carbon molecular sieve membranes (CMSM) in the form of hollow fibres [8] or flat sheets [1], and diamine as CO₂ absorber. High permeation and ideal selectivities for CO₂/Xe and N₂/Xe were obtained in the case of single gas experiments. On the other hand, multicomponent performance was adversely affected by Xe, that possesses a kinetic diameter of 4.04 Å, which is able to block the pores close to the CMSM surface (with diameters in the range of 3-5 Å) resulting in the reduction of the free pore space and limitation of the diffusion of other species. Hollow-fiber based non-volatile liquid membranes have been also successfully applied for CO₂ removal from N₂O anaesthesia mixtures containing halogenated hydrocarbons [9].

Recently, Yong *et al* (2016) have described the use of a hollow fibre membrane-based gas-liquid contactor for CO₂ capture using potassium carbonate as a solvent [10]. The authors propose the coating of the membrane surface, non-porous PDMS-PS or porous PP, with carbonic anhydrase (CA) enzyme by LbL technique to: i) increase mass transfer rates due to the reduction in pore wetting by the adsorbed polyelectrolytes; ii) to promote the CO₂ absorption kinetics into K₂CO₃. However, a slight loss in enzyme activity due to immobilization is observed even during the short term kinetic studies.

Additionally to all the trials focused on the membrane type, material and morphology, it was discovered that some ionic liquids possess high affinity towards CO₂ and the addition of carbonic anhydrase increases this property remarkably [11, 12]. CA is a naturally occurring thermoresistant metalloenzyme that works as a catalyst for the reversible conversion of CO₂ into bicarbonate (HCO₃⁻) at extremely high turnover rates. It regulates important biological processes within humans and other living organisms. This catalytic activity has been exploited for promoting the absorption of CO₂ from N₂ containing gas streams [12-14]. Neves *et al* (2012) described the use of supported liquid membranes for the integrated CO₂ capture and enzymatic bioconversion. A commercial hydrophobic porous membrane made of polyvinylidene fluoride (PVDF) was used as a support for the immobilization of CO₂ absorbing solvents, i.e. polyethylene glycol (PEG) 300 and 1-butyl-3-methylimidazolium bis(trifluoromethanesulfonyl) imide ionic liquid. The CO₂ solubility increased between 20% and 30%, even at low enzyme concentration (0.01% w/w) due to the chemical reaction enhancement factor [12].

In the last decade, biodegradable, biocompatible and environmental-friendly ILs that are synthesized by naturally-derived materials such as sugars and aminoacids are gaining increasing importance. This novel class of ILs may provide an optimum media to stabilize proteins (i.e. enzyme) [15] which is of our interest for the increase in CO₂ capturing effect. Cholinium cations are quaternary ammonium cations ([N,N,N - trimethylethanolammonium]⁺) fully derived from natural products [11, 16]. It was shown that the cholinium cations combined with a range of alkanoate anions or amino acids provide a media where living cells can actively grow [17, 18]. Moreover, they show high CO₂ capturing effect by absorption plus chemical reaction that take place due to their ammonium cations [19]. When compared to the commonly used ionic liquids for CO₂ capture [20], the CO₂ solubility values are lower, i.e. 0.209 mol/mol for 1-ethyl-3-methylimidazolium bis(trifluoromethylsulfonyl)imide compared to 0.152 mol/mol for cholinium propionate at 10 bar and 303 K. Nevertheless, cholinium based ILs show high biocompatibility and provide an environment where CA is active.

Martins *et al* (2016) evaluated the CO₂ solubility and diffusivity values in cholinium based ionic liquids as a function of water activity content and in the presence of CA (0.01% w/w). The highest CO₂ solubility was obtained at the lowest water activity due to the lower solubility of CO₂ in an ionic liquid with higher water content. However, in case of the ionic liquid combined with the enzyme, the highest enhancement in CO₂ solubility was obtained with the largest a_w because, under these conditions, the required water is available to assure the enzyme activity. As a result, the optimal water activity value was identified to be 0.753. Among the tested ILs, cholinium propionate (CP) exhibited the highest potential for CO₂ capture with a maximum transport enhancement of 63% in the presence of CA [11].

The present work pursues the proof of concept validation of a PDMS based microfluidic device as a gas – liquid contactor, with cholinium propionate and CA as a liquid phase, for the removal of CO₂ from Xe anaesthetic gas. A priori, the high gas permeability values of dense free standing PDMS membranes could allow to fully exploit the advantageous effect of the CO₂ enzymatic reaction in the liquid phase. In addition, due to miniaturization, the volume of ionic liquid required to fill the micro – chamber and the amount of CA are notably reduced while providing high throughput for the preliminary screening of different ionic liquid-enzyme formulations at several working conditions. Furthermore, this approach could be of interest for Xe recovery systems that require low capacity as is the case of recirculating machines for neonates. Moreover, the general advantages of PDMS microfluidic devices in terms of fabrication (simplicity and cost), weight, size, easy integration and scaling up by

replication and stacking by O₂ plasma are also worthy to mention. The microdevice consists of two independent chambers (one dedicated to the liquid phase and the second one devoted to the gas phase) and a non-porous flat PDMS membrane in between. The gas, CO₂ or Xe, is introduced in one of the chambers, permeates through the membrane and dissolves in the ionic liquid on the other compartment. An alveolar design has been mainly adopted for the liquid chamber to ensure that mass transfer of CO₂ through the liquid phase, in order to reach the CA active reaction sites, does not become rate controlling. As in previous works, enhanced CO₂ transport is expected due to the high solubility of CO₂ in cholinium propionate assisted by the enzymatic CO₂ conversion, both leading to greater driving force. In order to confirm such hypothesis the following tasks were performed: 1 – design and fabrication of a polymeric membrane and a microfluidic device with different geometries depending on the chamber purpose (liquid or gas); 2 – characterization of the fabricated chip in terms of leaks, membrane detachment and maximum tolerable pressure for its validation as G-L contactor; 3 – determination of the single gas permeability values of free standing membrane; and, 4 – evaluation of the G-L microcontactor performance for CO₂ capture due to the presence of CP solvent flowing in the liquid chamber and the use of CA to accelerate CO₂ transport.

2. Materials and methods

2.1. Materials

2.1.1. Ionic liquid tested

Cholinium propionate (CP) was used in the CO₂/Xe separation procedure. The ionic liquid was prepared by neutralization of propionic acid (purchased from Sigma-Aldrich, USA) in choline hydroxide. The resulting ionic liquid (IL) was equilibrated into a specific water activity, i.e. 0.753, with a sodium chloride salt (Applichem, Panreac, Germany). The water content corresponding to a given water activity was measured with a Karl-Fisher coulometer (Metrohm, model 831 KF coulometer).

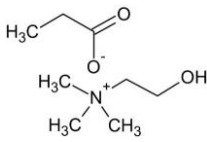
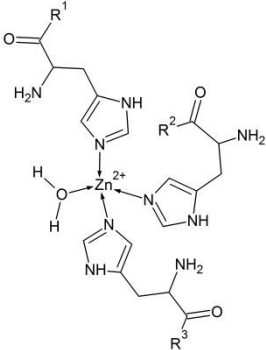
2.1.2. Carbonic anhydrase enzyme

Carbonic anhydrase (CA) lyophilized from bovine erythrocytes (ref: C3934, Sigma-Aldrich, USA), was used in this work without any further purification. 0.1 mg of the enzyme was added to 1 g of ionic liquid, and the resulting mixture was placed on the mixing plate till complete dissolution.

2.1.3. Ionic liquid and enzyme preparation

Taking into account that CO₂ is a Lewis acid, the absorbents which are chemically reactive with CO₂ are usually bases [19]. Thus, cholinium – based ionic liquids show high CO₂ capturing effect due to their ammonium cations. One of the parameters affecting the performance of the ionic liquids is their water activity (a_w). Henry’s constant, which is the inverse of gas solubility, increases with the increase of a_w. The water activity selected for the permeation experiments was equal to 0.753 based on the results obtained by Martins *et al* [11]. Table 1 shows the parameters of the ionic liquid and the enzyme selected for this work. The enzymatic activity of CA is derived from a Zn²⁺ ion that is coordinated to three histidine residues near the centre of the molecule in a cone-shaped cavity.

Table 1 Parameters of the liquid phase used for CO₂ capturing experiments

Ionic Liquid	Cholinium propionate (CP)	
Density [g·cm ⁻³]	1.07	
Molecular weight [g·mol ⁻¹]	177	
Viscosity [Pa·s]	0.039	
Water activity	0.753	
Water content [%]	35.7	
Henry Constant CO ₂ [bar]	65.59	
CO ₂ Diffusivity [m ² ·s ⁻¹]	3.3·10 ⁻¹⁰	
Ionic Liquid + Enzyme	Carbonic Anhydrase (CA)*	
CA conc in IL [mg·g ⁻¹ IL]	0.1	
Water activity	0.753	
Water content [%]	40.9	
Henry constant CO ₂ [bar]	74.23	

*the depicted chemical structure only corresponds to the central part of the molecule

2.1.4. Gases

The gases used in the experiments were xenon, Xe (purity grade 99.999%, Praxair, USA), carbon dioxide, CO₂ (high-purity grade 99.998% Praxair, USA) and oxygen, O₂ (purity grade 99.999%, Praxair, USA).

2.2. Methods

2.2.1. Design and fabrication of the PDMS chip

The microfluidic device used in this work was entirely made of Poly dimethyl siloxane (PDMS; Sylgard 184 Dow Corning, Midland, MI). PDMS was used due to its optical transparency, biocompatibility and mechanical properties which mean that it can be easily released from moulds and it conforms to surfaces. It consisted of two chambers, where one was dedicated to gas and the other to ionic liquid (CO₂ solvent). Both compartments were separated by a dense membrane (approximately 60 μm thick) made of the same material. The gas chamber, in the form of an empty reservoir, possessed a number of supporting pillars in order to reduce the risk of membrane and chip collapse. Liquid channels were arranged in a branching-like-architecture, including flow distributors, so the ionic liquid could circulate in a homogenous flow regime to reduce dead volume (see SI, Fig S1) and to avoid high pressure drop across the structure when dealing with high viscous fluids. Computer modelling in COMSOL Multiphysics 5.0 was done to calculate the pressure exerted on the walls of the liquid chamber for the CP ionic liquid at a liquid flow rate of 0.01 mL·min⁻¹. The estimated ΔP in the liquid chamber was equal to 0.14 mbar. Thus, the branching-like architecture allows to work with high viscous ionic liquids without the risk of pressure build up, channel blockage and chip collapse; unless fabrication defects or inadequate chip punching lead to obstructed channels. The depth of the liquid channel, i.e. 100 μm, also aimed to minimize mass transfer limitations in the permeate side.

The liquid as well as gas channel moulds were fabricated using a fabrication procedure reported previously by several authors [21-25] (See SI, Fig S2). Briefly, the masters were prepared by standard photolithography to create a pattern in SU-8 photoresist (SU-8 50 DE MicroChem) deposited on a flat silicon substrate (Fig 1 A-B). SU-8 is a commonly used epoxy-based negative photoresist, which is a light sensitive material, that is used to form a patterned coating usually on a silicon wafer surface. Next, PDMS pre-polymer and curing agent were thoroughly mixed in a ratio 10:1 and placed in the vacuum chamber for degassing. PDMS was poured on the masters and placed in the oven for 45 min at 80°C (Fig 1 C). The moulds were peeled off from the silicon wafer, cut to the required size and punched for inlet and outlet by a round punch (TiN Coated Round Punch, Syneo). Fabricated chambers were immersed in the solution of isopropanol (Sigma Aldrich) and placed in the ultrasound bath for approximately 2 minutes in order to remove any possible dust that could be attached to the inside of the channels or PDMS debris inside the punched holes prior any further procedure.

The PDMS membrane was made by spin coating (WS-400BZ, Laurell Technologies Corporation Spin Coater) on the surface of another wafer. The PDMS precursor solution was

placed on the wafer and spincoated at 1000 rpm during 1 minute resulting in a membrane thickness of 60 μm (Fig 1 D). The fabricated PDMS platform dedicated to liquid was placed inside the O_2 plasma chamber (Diener electronic, Plasma-surface-technology) operating at 0.4 mbar, 120 W and 50% of O_2 during 50 sec, in order to activate the surfaces, which will enable connecting the PDMS platform to the PDMS membrane [26] (Fig 1 E). After the surface was functionalized with O_2 plasma, the PDMS compartment was connected to the membrane and peeled off from the wafer. Next, the other platform was placed inside the O_2 plasma chamber, functionalized and connected to the other side of a membrane resulting in a microfluidic device made of two independent PDMS compartments (Fig 1 F). The fabricated chips were free of dust and other particles and both chambers were well attached to the membrane, no leaking was observed. Figure 1 A-F shows the process flow of the PDMS chip fabrication.

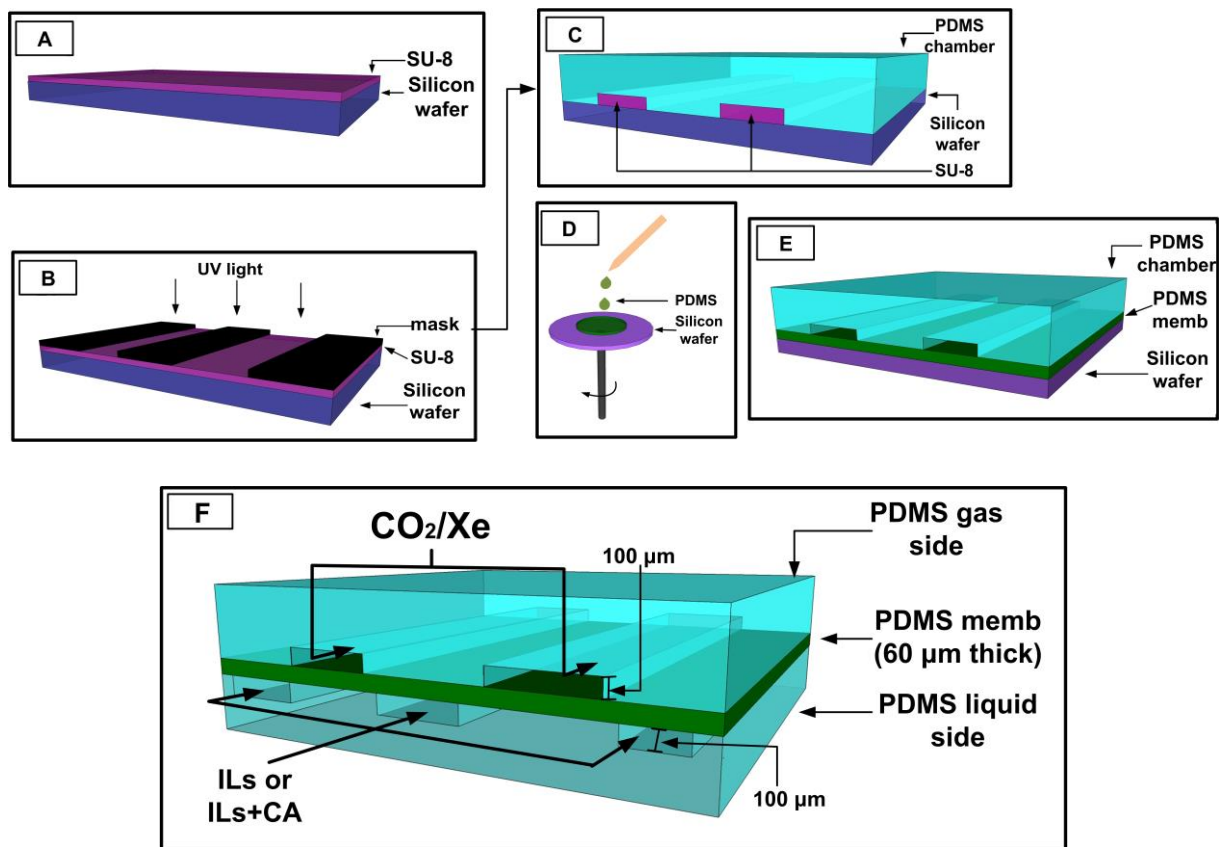


Figure 1 Process outline of the microfluidic chip fabrication. SU-8 negative photoresist was spin coated on the silicon wafer (A), mask alignment, UV exposure and SU-8 development (B), PDMS was poured on a created mould (C) and peeled off after curing. The membrane was prepared by spin coating on a silicon wafer (D) and connected to the PDMS mould by O_2 plasma procedure (E). After curing in the oven, the membrane and the chamber was peeled off of the wafer and connected to the other chamber (F).

2.2.2. Characterization of the microfluidic device

The liquid chamber architecture enabled uniform flow of the ionic liquid through the branching construction of the microchannels while capturing CO₂ permeating through the PDMS membrane. Use of PDMS elastomer facilitated chip fabrication and reproduction of the same design with thin non-porous membrane attached to the chambers. Four replica of the same design were fabricated. All of them possess a membrane of approximately 60 μm thickness, but slightly differ in the thickness of the PDMS mould compartment, varying from 0.8 to 1 cm due to the fabrication procedure. The four chips were built and tested; each device was capable to work for many hours under the conditions indicated below.

Figure 2 A shows the photograph of a microchip with the liquid chamber filled with blue dye and the gas compartment filled with pink dye to visualize the flow path. The image indicates that the filling of the gas and liquid channels was homogenous, demonstrating that there was no dead volume. Metallic pins (precision stainless steel dispense tips from Nordson, The Netherlands) with outer diameter of 0.025” and gauge 23 were inserted at the inlet and outlet of gas and liquid compartments to facilitate introduction of the piping into the microchip. Metallic pins and piping also contribute to the increase of a pressure drop across the entire system. To avoid deformations or leaks in the chip the maximum allowable pressure in the gas side was 0.1 bar. On the other hand, the maximum allowable liquid flow rate was equal to 0.01cm³·min⁻¹, leading to the pressure drop of the liquid side, considering piping, pins and the chamber, to approximately 6 mbar. The SEM (CSEM-FEG INSPECT F50) picture of a cross section of the microdevice was taken after coating the PDMS with platinum by low vacuum coater (Leica EM ACE200). Figure 2 B indicates that the membrane is well attached to the microfluidic chambers.

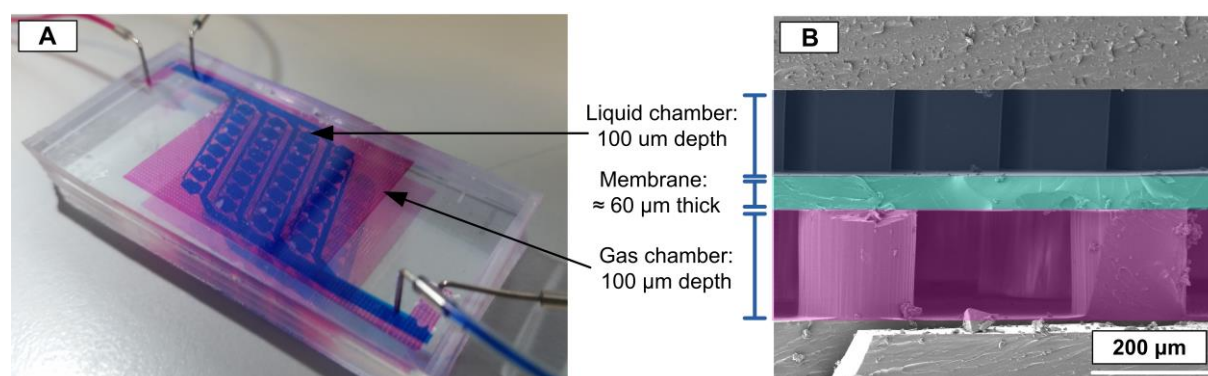


Figure 2 PDMS microfluidic device (A) with food dye for better visualisation of liquid and gas chamber and (B) SEM image of a microchip cross section

The volume of the gas chamber was equal to 0.073 cm³ and volume of the liquid was 0.038 cm³, while the depth of each chamber was equal to 100 μm. The chip footprint, defined

as the total size of the microfluidic device taking into account its width and length, was equal to 18.9 cm² making it a very compact system. The membrane surface area was 3.87 cm², resulting in a 3500 m⁻¹ S/V_{liquid+gas} ratio.

2.2.3. Single gas permeation experiments on PDMS membranes

Firstly, the permeability of a free-standing PDMS membrane was evaluated, according to the method previously described by Neves *et al* [12]. The system was composed of a gas source, gas compartment, pressure transducers (Druck PDCR 910 models 99166 and 991675, England) and temperature controller which was immersed in a water bath. The stainless-steel cell was made of two identical chambers (6 cm³) dedicated to the feed and permeate with the membrane in between. The stainless-steel cell was placed in a water bath at 30°C. The permeability of three different pure gases was measured: CO₂, O₂ and Xe. The identical compartments were pressurized with pure gas, and after opening the permeate outlet (see Fig S3 in SI) a pressure difference of about 0.7 bar was imposed. The pressure decay on the feed side and the pressure increase on the permeate side were recorded using two pressure transducers.

2.2.4. Single gas permeation experiments on microfluidic devices containing ionic liquids and enzyme

The experiments with ionic liquids were carried out in the experimental system shown in Fig 3. In this case, there was one pressure transducer connected to the gas chamber while the ionic liquid, without and with the enzyme, was fed by a syringe pump connected to the liquid chamber, i.e. permeate side, at 0.01 cm³·min⁻¹. The outlet of the liquid side was left open to the atmosphere so there was always a fresh portion of ionic liquid entering the compartment. The permeation of Xe and CO₂ was measured. The gas compartment was pressurized up to approximately 0.1 bar. After equilibrium, valve V3 was opened while all the other valves were closed. The temperature was kept constant at 30°C.

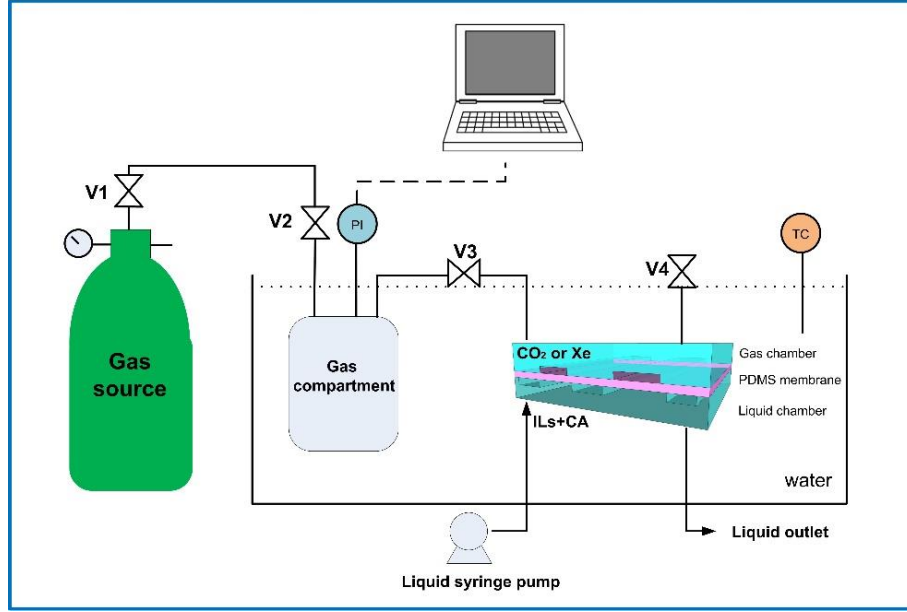


Figure 3 Experimental system for measuring the transport rate of CO₂ and Xe in the presence of ionic liquid and ionic liquid containing carbonic anhydrase

2.3. Calculations

The equations presented below were used for calculating the permeability of a free-standing membrane. Moreover, the global mass transfer coefficients were also calculated for the chip under operation with the liquid compartment filled with ionic liquid or with ionic liquid and enzyme. The equations and assumptions used are presented below.

2.3.1. Gas permeability calculation of a free-standing membrane

Single gas permeability of a free standing membrane was calculated according to expression (1), which was derived from the mass balance equation under non-steady state conditions [27] as described by Neves *et al* [12]:

$$\frac{1}{\beta} \ln \left(\frac{[P_{feed} - P_{perm}]_0}{[P_{feed} - P_{perm}]} \right) = p \frac{t}{l} \quad (1)$$

where P_{feed} and P_{perm} are the pressures in the feed and permeate side, respectively [bar], t is time [s], l corresponds to the membrane thickness [m], p is the membrane permeability [$m^2 s^{-1}$] and β [m^{-1}] is a parameter which depends from the geometry of the compartment and is given by:

$$\beta = A \left(\frac{1}{V_{feed}} + \frac{1}{V_{perm}} \right) \quad (2)$$

where V_{feed} and V_{perm} are the volumes of the feed and permeate chambers, respectively [m^3], and A is the membrane surface area [m^2]. In the experimental system used for our measurements the value of β was equal to 106.38 [m^{-1}]. The conversion of permeability expressed in $m^2 s^{-1}$, into units of barrer is described in detail in [27].

The permeability of the free-standing membrane, calculated by the presented method, was used for the evaluation of individual resistances in the liquid phase (see section below).

2.3.2. Calculation of Global Mass Transfer Coefficient, Individual Resistances and Enhancement Factor

The flux of CO_2 , denoted as J [$mol \cdot m^{-2} \cdot s^{-1}$], from the gas to the liquid side in a membrane contactor is governed by equation (3):

$$J = K \Delta C = K(C_G - C_G^*) \quad (3)$$

where K [$m \cdot s^{-1}$], is the overall mass transfer coefficient for CO_2 transport, ΔC is the driving force: C_G is the concentration of CO_2 in the gas phase and C_G^* is the concentration of CO_2 in the gas phase that is in equilibrium with the CO_2 concentration in the bulk liquid phase. Under the experimental conditions chosen for the evaluation of K_{CO_2} , the hypothetical concentration of CO_2 in equilibrium with the CO_2 dissolved in the ionic liquid (C_G^*), can be considered negligible due to the CO_2 Henry constant value of the selected cholinium-based ionic liquid (see Table 1) and the continuous feeding of fresh ionic liquid to the chip ($0.01 \text{ cm}^3 \cdot \text{min}^{-1}$).

The mass transfer coefficient for the ionic liquid or ionic liquid with enzyme was calculated from the exponential fit of the normalized pressure decay curve based on equation (4):

$$-V \frac{dC_G}{dt} = K \cdot A \cdot (C_G - C_G^*) \quad (4)$$

where, A is the membrane surface area [cm^2].

The overall mass transfer coefficient for gas transport in a G-L membrane contactor can be described by the resistance in series model as shown below in equation (5):

$$\frac{1}{K} = \frac{1}{k_G} + \frac{1}{k_M} + \frac{1}{mEk_L^0} \quad (5)$$

where k_G is the individual mass transfer coefficient in the gas phase [$\text{m}\cdot\text{s}^{-1}$], k_M is the individual mass transfer coefficient associated with transport through the membrane [$\text{m}\cdot\text{s}^{-1}$], k_L^0 is the individual liquid phase mass transfer coefficient [$\text{m}\cdot\text{s}^{-1}$] in absence of chemical reaction, i.e without the CA enzyme, m is the Henry's law constant [-] and E is the enhancement factor due to the enzymatic reaction [-] which can be expressed as in equation 6 for first order reactions, which is reasonable to assume because the enzyme is far from being saturated:

$$E = \frac{Ha}{\tanh(Ha)} \quad (6)$$

where Ha is the Hatta number which relates the overall absorption rate to the physical absorption rate of CO_2 .

The membrane resistance (R_M) is calculated simply by the inverse of the individual mass transfer coefficient inside the membrane ($\frac{1}{k_M}$). Similarly, the resistances resulting from the presence of ionic liquid (R_{CP}) or ionic liquid with the enzyme (R_{CP+CA}) are calculated from the inverse of the mass transfer coefficient of the IL ($\frac{1}{mk_L^0}$) and mass transfer coefficient with the enzyme ($\frac{1}{mEk_L^0}$) respectively.

The overall mass transfer coefficient expression can be simplified further to be solely dependent on k_M and k_L^0 because all the experiments herein performed have been carried out with pure gases resulting in:

$$\frac{1}{K} = \frac{1}{k_M} + \frac{1}{mEk_L^0} \quad (7)$$

3. Results and discussion

3.1 Permeability of a Free – Standing Membrane

Figure 4 shows the normalized $\Delta P/\Delta P_0$ decay (defined using $t=0$ as reference) as a function of time divided by the membrane thickness, for two different free-standing membranes (60 μm thick and 126 μm thick). The measurements were performed for O_2 , Xe and CO_2 . The raw data (see Fig S4, SI) shows that the pressure decrease of the feed is equal to the increase of pressure at the permeate indicating that the volumes of the feed and permeate chambers are identical. As it was expected, the slowest $\Delta P/\Delta P_0$ decrease is observed in case of O_2 which has the lowest permeability through the PDMS membrane and the fastest decrease is detected for CO_2 , which has the highest permeability through PDMS. This is in agreement with previous findings [28] and technical information provided by PDMS membrane suppliers. In all the cases, the mass balance is satisfied within $\pm 5\%$.

The objective of the experiment with a free-standing membrane was to validate the experimental system, confirm the calculation procedure and to compute the permeability of the spin – coated non – commercial PDMS membranes (See Table 2). There are several factors influencing the permeation through PDMS membranes, being the two most important ones the mixing ratio and curing temperature during membrane preparation. The mixing ratio of the PDMS prepolymer to the curing agent used in this work was 10:1. This ratio is suggested by the polymer provider and leads to a good balance between permeability and mechanical stability of the material. In general, a higher amount of cross–linker leads to a more mechanically stable structure with lower permeability [29-32]. Thus, the optimal prepolymer: curing agent ratio depends on the final application.

Table 2 O_2 , CO_2 and Xe permeability values calculated for the prepared free-standing membranes

Thickness [μm]	Permeability O_2 [barrer]	Permeability CO_2 [barrer]	Permeability Xe [barrer]	Ideal Selectivity $\alpha_{\text{CO}_2/\text{Xe}}$
60	357	854	620	1.4
126	310	843	612	1.4

Additionally, it is concluded from Table 2 that the permeability of Xe is only slightly lower than that of CO_2 with an ideal selectivity of 1.4. In fact, the values of the Lennard – Jones kinetic diameters are similar, 3.94 \AA and 4.04 \AA for CO_2 and Xe, respectively [33]. Merkel *et al* [28] studied the permeability of different gases in PDMS and they concluded that, even though the kinetic diameters of gases are similar, permeabilities can be different as a result of relative solubility of a gas in PDMS. Typically, gases with higher critical temperatures, such as CO_2 , exhibit high condensability and are more soluble in polymers as well as in liquids.

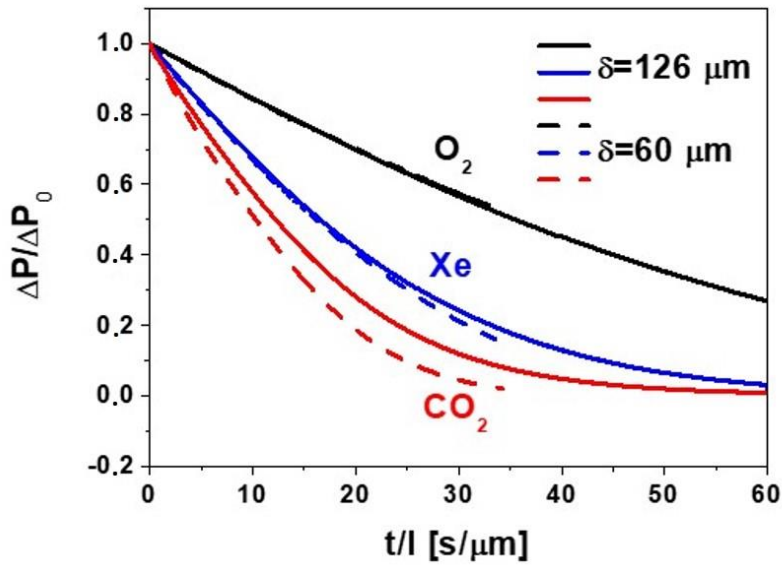


Figure 4 Normalized pressure drop in the experiments with three different gases (O_2 , Xe and CO_2) for two distinctive free-standing membranes (60 μm thickness and 126 μm thickness).

3.2 Gas transport in the microfluidic device

The gas permeation experiments through the membrane integrated in the microfluidic chip were carried out in the experimental system shown in Figure 3. In this case, the liquid chamber was empty and the valves connecting the chamber to the atmosphere were closed. The pressure decay was recorded for Xe and CO_2 . Figure 5 shows the comparison of normalized pressure drop for four different chips in the case of CO_2 .

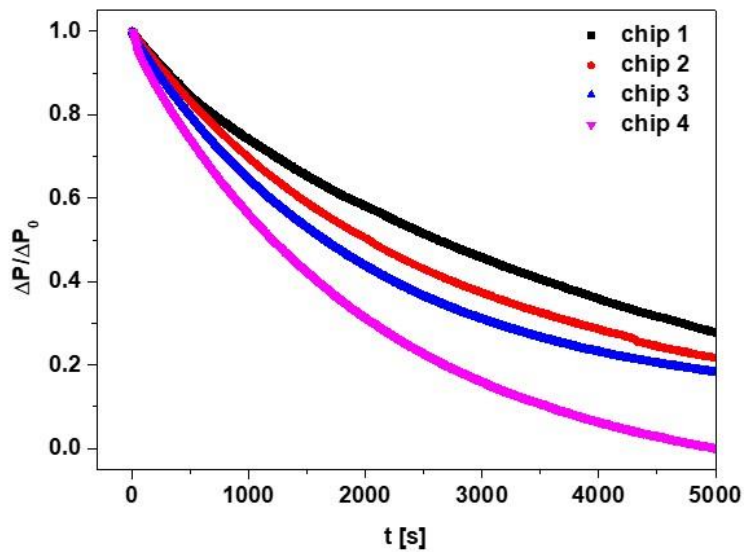


Figure 5 Normalized pressure drop of CO_2 in the four different chips

For raw data of the pressure decrease at the feed side and pressure increase at the permeate side for CO₂ inside one of the chips, see Fig S5, SI. The pressure in the feed side decreases slower than the pressure at the permeate increases. This is related to the difference in the volume of the two chambers. Considering that the feed chamber consists of a gas compartment made of a stainless steel connected to the gas side of the microdevice and accounting for all the connections, the total volume of the feed side is 72.83 cm³. On the other hand, the permeate side consists only of a liquid chamber of the microfluidic device and the piping resulting in a volume of 0.12 cm³. Additionally, in the proposed microdevice there is not only a membrane which is made of PDMS but also both chambers. Unlike free-standing membrane experiments, the amount of CO₂ moles permeating from the feed side significantly differed from the amount of CO₂ moles appearing on the permeate side. The contribution of CO₂ sorption on the PDMS side walls accounts for up to 15%. In other words, the gas permeates not only through the membrane but through the chamber walls as well, resulting in modified gas transport values. In this scenario, a significant contribution of the PDMS walls effect on the recorded pressure variation in the feed side is expected. To corroborate such hypothesis, the CO₂ permeability measurements of chip 4 were carried out slightly different: before the pressure decay measurement, the microfluidic device was saturated with CO₂ for about 3 hours. After that time, the measurement was performed as it was described above. The purpose of this procedure was to saturate the PDMS walls with CO₂. Therefore, the total transport of CO₂ occurred in the membrane rather than in the PDMS walls. This is visible in Figure 5 where the highest decay of the normalized pressure is observed in Chip 4. Hence, it was decided that to avoid the contribution of the PDMS walls in the gas permeation, the values of the PDMS membrane permeability and a membrane resistance for a given gas will be taken from the experiments presented in the previous section for a free – standing membrane (see Table 2) rather than from the measurements of gas permeation in the membrane integrated in the chip.

3.3 CO₂ transport enhancement due to cholinium propionate ionic liquid and carbonic anhydrase enzyme

To increase the CO₂ capturing effect, cholinium propionate ionic liquid, CP, alone or combined with the carbonic anhydrase enzyme, CA, was introduced in the liquid chamber by a syringe pump with the flow rate of 0.01 cm³.min⁻¹ (see Figure 3). The experiments were

carried out for four different chips with PDMS dense membrane, 60 μm thick. However, in order to ensure the selectivity of the process, which is the separation of CO_2 from Xe in an anaesthesia gas stream, the transport of Xe in presence of cholinium propionate and cholinium propionate combined with carbonic anhydrase has to be investigated. Therefore, the same set of experiments were carried out in the case of Xe. As it was done in the previous measurements, pressure decay of the analysed gas was recorded and the calculation of the resistance of each process as well as the mass transfer coefficients were performed.

Figure 6 shows the normalized pressure decay in the feed side for all three experimental configurations as a function of time for CO_2 (A) and Xe (B), respectively. There is no visible effect of ionic liquid and the enzyme on the affinity to Xe, in comparison to the measurements with the empty liquid chamber. Accounting from preliminary results of Xe solubility in bulk cholinium propionate ionic liquid, i.e. negligible [11] (see Figure S6 in SI), the Xe pressure decay profiles depicted in Figure 6b could be explained by the contribution of Xe sorption on the walls of the PDMS chambers.

On the other hand, there is a slight enhancement in the pressure decay in case of CO_2 and ionic liquid. The CO_2 pressure decreases even more rapidly as a result of the enzymatic reaction, i.e. due to the presence of the enzyme in the ionic liquid. Figure 7 represents the final decay of pressure in the feed side of the four different chips. The normalized pressure decay of the four chips is presented in the supplementary information (SI, Fig S7). It is visible that the ionic liquid has an influence on the CO_2 transport and it increases it moderately. However, a significant increase in CO_2 transport is obtained when the enzyme is added to the IL, which is in agreement with previous works and results obtained by Martins *et al* for the immobilization of carbonic anhydrase in cholinium propionate in a bulk system [11].

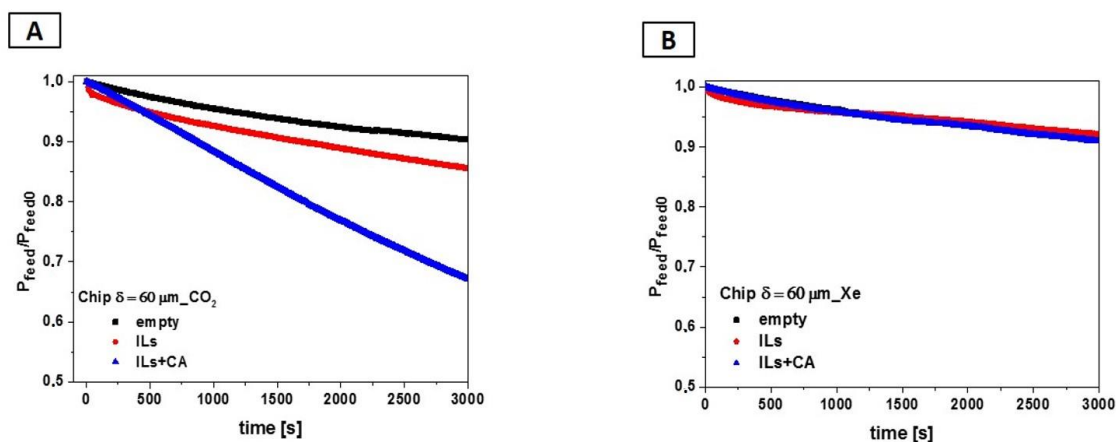


Figure 6 Normalized pressure decay in the feed side over time in the empty chip 1 (no IL), the chip 1 with cholinium propionate and the chip 1 filled with cholinium propionate and carbonic anhydrase for CO_2 (A) and Xe (B).

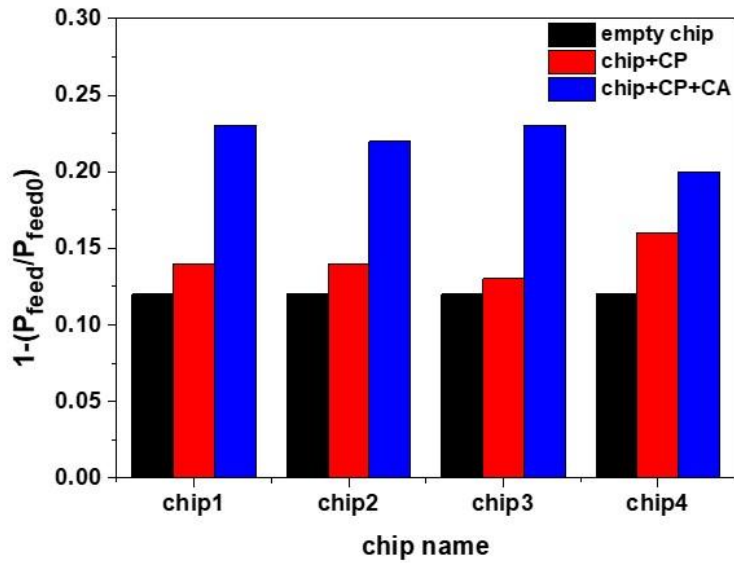


Figure 7 Enhanced CO₂ transport due to the presence of ionic liquid and the enzyme in the liquid chamber: results for the 4 different chips prepared in this work.

The individual mass transfer coefficient for transport through the membrane, k_M , and the global mass transfer coefficients for CO₂ transport, K_{CO_2} with ionic liquid and with ionic liquid combined with the enzyme are presented in Table 3. The mass transfer coefficient for the membrane, k_M is calculated by dividing the permeability value by the thickness of each membrane integrated in the microfluidic device. The global mass transfer coefficients for CO₂ transport, K_{CO_2} is calculated from equation (4). In the case of Xe, the calculation of the overall mass transfer coefficient cannot be performed following the same procedure since there is not a measurable absorption of Xe in the ionic liquid. Table 3 also shows the enhancement factor, as well as, the molar flux ratio between CO₂ and Xe, i.e. J_{CO_2}/J_{Xe} .

Table 3 Mass transfer coefficients, resistances and enhancement factor for CO₂ transport in cholinium propionate and cholinium propionate combined with carbonic anhydrase. R_{CP} is the resistance in the ionic liquid, R_{CP+CA} is the resistance in the ionic liquid combined with the enzyme, E is the enhancement factor due to the chemical reaction.

	Chip	Chip+CP		Chip+CP+CA			
Chip	$K_{CO_2} = k_M$ [m·s ⁻¹]	$K_{CO_2} = \frac{1}{\frac{1}{k_M} + \frac{1}{m k_L^0}}$ [m·s ⁻¹]	R _{CP} [%]	$K_{CO_2} = \frac{1}{\frac{1}{k_M} + \frac{1}{m E k_L^0}}$ [m·s ⁻¹]	R _{CP+CA} [%]	E	J _{CO₂} /J _{Xe}
1	1.19·10 ⁻⁵	1.24·10 ⁻⁶	89.6	2.11·10 ⁻⁶	82.3	1.9	3.5
2	1.17·10 ⁻⁵	1.25·10 ⁻⁶	89.3	2.07·10 ⁻⁶	82.3	1.8	2.9
3	1.10·10 ⁻⁵	1.58·10 ⁻⁶	85.6	2.11·10 ⁻⁶	80.8	1.4	3.8
4	1.14·10 ⁻⁵	1.51·10 ⁻⁶	86.8	1.87·10 ⁻⁶	83.6	1.3	3.0

Above all, the results obtained indicate that the main controlling resistance to CO₂ transport in the gas – liquid membrane contactor is located in the liquid phase. We found that individual liquid phase resistance values, R_{CP}, are in the range of 86-90% of the total resistance. The overall mass transfer coefficients are two orders of magnitude lower than the ones presented by Yong *et al* due to the higher viscosity of the ionic liquid (39 mPa·s vs 2 mPa·s) and the much lower solvent Reynolds number (0.001 vs. 20) used in this work. Additionally, in our case, it was decided to not increase the flow rate of the IL because this would augment the pressure drop in the entire system, above the limit of 0.1 bar, leading to deformation and leaks in the chambers. The enhancement factor on CO₂ transport due to the presence of the enzyme increases up to an average value of 1.6. This value is rather positive when compared with published results [10], in particular if we take into consideration the low enzymatic concentration used in the microfluidic device, i.e. 0.1 mgCA/gIL. The enhancement factor (E) results, after addition of carbonic anhydrase to the cholinium propionate ionic liquid, are in agreement with the results obtained by Martins *et al.* for bulk experiments [11], where an enhancement factor of 1.6 was also obtained. This observation supports the benefits of the alveolar type design for ensuring the facile access of CO₂ to the CA active reaction sites. Moreover, the CO₂/Xe molar flux ratio after addition of the ionic liquid and the enzyme is as high as 3.3 compared to 1.4 ideal selectivity obtained using the PDMS membrane.

Since there is no Xe absorption by the ionic liquid it can be totally recycled in a closed anaesthetic circuit as represented in Figure 8.

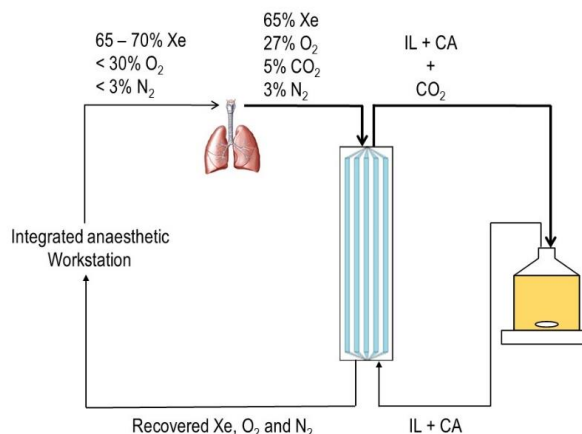


Figure 8 Simplified scheme for CO₂ removal and Xe recycling in a closed anaesthetic circuit

4. Conclusions

In summary, we have investigated the effect of an ionic liquid and its combination with carbonic anhydrase to remove CO₂ from Xe used in anaesthesia. The microfluidic experimental system was designed as a membrane contactor working in a semi-continuous operation mode. Even though the permeability of PDMS for Xe and CO₂ was similar, the cholinium propionate and cholinium propionate in combination with carbonic anhydrase showed the enhancement in the CO₂ capturing effect, while there was no effect on the Xe transport rate.

Our work demonstrates the proof of concept for CO₂ removal from anaesthesia gas circuits through a membrane contactor in the form of a microfluidic device. Thanks to miniaturization, the consumption of chemicals, i.e. ionic liquid and enzyme, is notably reduced. At the same time, it provides a significant enhancement factor and molar flux ratio of CO₂/Xe using very small concentration of CA enzyme 0.1 mgCA/gIL.

Further research should also consider: i) alternative non-permeable materials with higher mechanical resistance for the fabrication of the microfluidic chambers; ii) exploring novel membrane architectures (porous, corrugated) to increase the S/V ratio; and, iii) use of higher concentrations of the CA enzyme and solvent flow-rates for promoting CO₂ transport.

Acknowledgments

The authors would like to acknowledge the financial support from the Government of Aragon and the Education, Audiovisual and Culture Executive Agency (EU-EACEA) within the EUDIME – “Erasmus Mundus Doctorate in Membrane Engineering” program (FPA 2011-0014, SGA 2012-1719, <http://eudime.unical.it>). CIBER-BBN is an initiative funded by the VI National R&D&I Plan 2008–2011 financed by the Instituto de Salud Carlos III with the assistance of the European Regional Development Fund. Authors acknowledge the LMA-INA for offering access to their instruments and expertise. This work was also supported by the Associate Laboratory for Green Chemistry LAQV which is financed by national funds from FCT/MEC (UID/QUI/50006/2013) and co-financed by the ERDF under the PT2020 Partnership Agreement (POCI-01-0145-FEDER-007265). Carla F. Martins acknowledge FCT for fellowship SFRH/BD/111128/2015 and Luísa A. Neves for the exploratory project grant IF/00505/2014/CP1224/CT0004 attributed within the 2014 FCT Researcher Program.

References:

1. S. Lagorsse, F.D. Magalhães, and A. Mendes, Xenon recycling in an anaesthetic closed-system using carbon molecular sieve membranes, *Journal of Membrane Science*, 301 (2007) 29-38.
2. K. Hecker, J.H. Baumert, N. Horn, and R. Rossaint, Xenon, a modern anaesthesia gas, *Minerva Anestesiologica*, 70 (2004) 255-260.
3. S.C. Cullen and E.G. Gross, The anesthetic properties of xenon in animals and human beings, with additional observations on krypton, *Science*, 113 (1951) 580-582.
4. S. Singh, Xenon: A modern anaesthetic, *Healthcare Management*, (2005).
5. S. D. Faulkner, N. A. Downie, Ch. J. Mercer, S. A. Kerr, R. D. Sanders, and N.J. Robertson, A xenon recirculating ventilator for the newborn piglet: developing clinical applications of xenon for neonates, *European Journal of Anaesthesiology*, 29 (2012) 577-585.
6. T. Goto, Is there a future for xenon anesthesia, *Canadian Journal of Anesthesia*, 49 (2002) 335-338.
7. E.J. Frink Jr, W.B. Green Jr, E.A. Brown, M. Malcomson, L.C. Hammond, F.G. Valencia, and B.R. Brown Jr, Compound A concentrations during sevoflurane anesthesia in children, *Anesthesiology*, 84 (1996) 566-571.
8. A. Mendes, Development of an adsorption/membrane based system for carbon dioxide, nitrogen and spur gases removal from a nitrous oxide and xenon anaesthetic closed loop, *Applied Cardiopulmonary Pathophysiol*, 9 (2000) 156-163.
9. G. Obuskovic and K.K. Sirkar, Liquid membrane-based CO₂ reduction in a breathing apparatus, *Journal of Membrane Science*, 389 (2012) 424-434.
10. J.K.J. Yong, G.W. Stevens, F. Caruso, and S.E. Kentish, In situ layer-by-layer assembled carbonic anhydrase-coated hollow fiber membrane contactor for rapid CO₂ absorption, *Journal of Membrane Science*, 514 (2016) 556-565.
11. C.F. Martins, L.A. Neves, M. Estevão, A. Rosatella, V.D. Alves, C.a.M. Afonso, J.G. Crespo, and I.M. Coelho, Effect of water activity on carbon dioxide transport in cholinium-based ionic liquids with carbonic anhydrase, *Separation and Purification Technology*, 168 (2016) 74-82.

12. L.A. Neves, C. Afonso, I.M. Coelho, and J.G. Crespo, Integrated CO₂ capture and enzymatic bioconversion in supported ionic liquid membranes, *Separation and Purification Technology*, 97 (2012) 34-41.
13. J. Hou, M. Y. Zulkifli, M. Mohammad, Y. Zhang, A. Razmjou, V. Chen, Biocatalytic gas-liquid membrane contactors for CO₂ hydration with immobilized carbonic anhydrase, *Journal of Membrane Science*, 520 (2016) 303-313.
14. W.C. Floyd, S.E. Baker, C.A. Valdez, J.K. Stolaroff, J.P. Bearinger, J.H. Satcher, and R.D. Aines, Evaluation of a carbonic anhydrase mimic for industrial carbon capture, *Environmental Science and Technology*, 47 (2013) 10049-10055.
15. X. Jia, Y. Yang, C. Wang, C. Zhao, R. Vijayaraghavan, D.R. Macfarlane, M. Forsyth, and G.G. Wallace, Biocompatible ionic liquid-biopolymer electrolyte-enabled thin and compact magnesium-Air batteries, *ACS Applied Materials and Interfaces*, 6 (2014) 21110-21117.
16. J.K. Blusztajn, Choline, a vital amine, *Science*, 281 (1998) 794-795.
17. M. Petkovic, J.L. Ferguson, H.Q.N. Gunaratne, R. Ferreira, M.C. Leitão, K.R. Seddon, L.P.N. Rebelo, and C.S. Pereira, Novel biocompatible cholinium-based ionic liquids - Toxicity and biodegradability, *Green Chemistry*, 12 (2010) 643-649.
18. F.A. E Silva, F. Siopa, B.F.H.T. Figueiredo, A.M.M. Gonçalves, J.L. Pereira, F. Gonçalves, J.a.P. Coutinho, C.a.M. Afonso, and S.P.M. Ventura, Sustainable design for environment-friendly mono and dicationic cholinium-based ionic liquids, *Ecotoxicology and Environmental Safety*, 108 (2014) 302-310.
19. C. Wu, T.P. Senftle, and W.F. Schneider, First-principles-guided design of ionic liquids for CO₂ capture, *Phys. Chem. Chem. Phys*, 14 (2012) 13163-13170.
20. E. Torralba-Calleja, J. Skinner and D. Gutierrez-Tauste, CO₂ Capture in Ionic Liquids: A Review of Solubilities and Experimental Methods, *Journal of Chemistry*, 2013 (2013) 16.
21. T. Kniazeva, A.A. Epshteyn, J.C. Hsiao, E.S. Kim, V.B. Kolachalama, J.L. Charest, and J.T. Borenstein, Performance and scaling effects in a multilayer microfluidic extracorporeal lung oxygenation device, *Lab on a Chip*, 12 (2012) 1686-1695.
22. J.T. Borenstein, H. Terai, K.R. King, E.J. Weinberg, M.R. Kaazempur-Mofrad, and J.P. Vacanti, Microfabrication technology for vascularized tissue engineering, *Biomedical Microdevices*, 4 (2002) 167-175.
23. B.G. Subramani and P.R. Selvaganapathy, Surface micromachined PDMS microfluidic devices fabricated using a sacrificial photoresist, *Journal of Micromechanics and Microengineering*, 19 (2009).
24. D.M. Hoganson, H.I. Pryor, E.K. Bassett, I.D. Spool, and J.P. Vacanti, Lung assist device technology with physiologic blood flow developed on a tissue engineered scaffold platform, *Lab on a Chip - Miniaturisation for Chemistry and Biology*, 11 (2011) 700-707.
25. N. Rochow, E.C. Chan, W.I. Wu, P.R. Selvaganapathy, G. Fusch, L. Berry, J. Brash, A.K. Chan, and C. Fusch, Artificial placenta - Lung assist devices for term and preterm newborns with respiratory failure, *International Journal of Artificial Organs*, 36 (2013) 377-391.
26. S. Bhattacharya, A. Datta, J.M. Berg, and S. Gangopadhyay, Studies on surface wettability of poly(dimethyl) siloxane (PDMS) and glass under oxygen-plasma treatment and correlation with bond strength, *Journal of Microelectromechanical Systems*, 14 (2005) 590-597.
27. E.L. Cussler, *Diffusion. Mass Transfer in Fluid Systems*, third edition, Press Syndicate of The University of Cambridge, Cambridge, (2009).
28. V.I.B. T. C. Merkel, K. Nagai, B. D. Freeman, I. Pinnau, Gas sorption, diffusion, and permeation in poly(dimethylsiloxane), *Journal of Polymer Science: Part B: Polymer Physics*, 38 (2000) 415-434.
29. A. Lamberti, S.L. Marasso, and M. Cocuzza, PDMS membranes with tunable gas permeability for microfluidic applications, *RSC Advances*, 4 (2014) 61415-61419.

30. A. Singh, B.D. Freeman, and I. Pinnau, Pure and mixed gas acetone/nitrogen permeation properties of polydimethylsiloxane [PDMS], *Journal of Polymer Science, Part B: Polymer Physics*, 36 (1998) 289-301.
31. K. Khanafer, A. Duprey, M. Schlicht, and R. Berguer, Effects of strain rate, mixing ratio, and stress-strain definition on the mechanical behavior of the polydimethylsiloxane (PDMS) material as related to its biological applications, *Biomedical Microdevices*, 11 (2008) 503.
32. M. Liu, J. Sun, and Q. Chen, Influences of heating temperature on mechanical properties of polydimethylsiloxane, *Sensors and Actuators, A: Physical*, 151 (2009) 42-45.
33. B.E. Poling, J.M. Prausnitz, and J.P. O'connell, *The properties of gases and liquids*, fifth edition, (2004).